Realization of the kicked atom at high scaled frequencies

C. O. Reinhold,[1,2] S. Yoshida,[3] J. Burgdörfer,[3,2] W. Zhao,[4] J. J. Mestayer,[4] J. C. Lancaster,[4] and F. B. Dunning[4]
[1]*Physics Division, Oak Ridge National Laboratory, Oak Ridge, Tennessee 37831-6372, USA*
[2]*Department of Physics, University of Tennessee, Knoxville, Tennessee 37996-1200, USA*
[3]*Institute for Theoretical Physics, Vienna University of Technology, A-1040 Vienna, Austria*
[4]*Department of Physics and Astronomy, and the Rice Quantum Institute, Rice University, MS 61, 6100 Main Street, Houston, Texas 77005-1892, USA*
(Received 19 January 2006; published 24 March 2006)

The response of quasi-one-dimensional very-high-n Rydberg atoms to a periodic train of short unidirectional electric-field pulses, termed half-cycle pulses (HCPs), is studied at high scaled frequencies. Pronounced nonmonotonic structure in the survival probability is observed as N, the number of HCPs in the train is increased, the survival probability actually increasing with N over certain ranges of N. This behavior is very sensitive to the polarization of the Rydberg states and is explained with the aid of classical simulations.

DOI: 10.1103/PhysRevA.73.033420 PACS number(s): 32.80.Rm, 32.80.Qk, 32.60.+i

I. INTRODUCTION

Earlier work has shown that the kicked Rydberg atom, i.e., a Rydberg atom subject to a train of identical equispaced unidirectional electric-field pulses, termed half-cycle pulses (HCPs), of duration $T_p \ll T_n$, where $T_n = 2\pi n^3$ (a.u.) is the classical electron orbital period, provides an excellent laboratory to study nonlinear dynamics in Hamiltonian systems [1–3]. Previous experiments, which were limited to scaled frequencies $\nu_0 = \nu_T/\nu_n < 3$ where ν_T is the frequency of the HCPs in the train and $\nu_n = 1/T_n$ is the classical electron orbital frequency, revealed a number of interesting phenomena including dynamical stabilization [3] and population trapping near the continuum [4]. Theory, however, suggests that at higher scaled frequencies interesting effects should be observed, including nonmonotonic decay of the survival probability as the number of HCPs in the train is increased. Moreover, the breakdown of classical-quantum correspondence as a result of quantum localization, the quantum suppression of classically chaotic ionization [5,6], is expected.

Experimental studies at high scaled frequencies pose substantial challenges. Trains of true unidirectional HCPs can be generated by applying the output of a fast pulse generator to a suitable electrode. While this allows precise control of the HCP train, the widths of the HCPs are typically limited to values $\gtrsim$500 ps with pulse repetition frequencies ν_T below 500 MHz. Since the orbital period is given by $T_n = (n/187)^3$ ns, scaled frequencies of the order of $\nu_0 \sim 10$ can only be explored by working with Rydberg atoms with very large values of principal quantum number n, $n \gtrsim 500$. Such atoms are difficult to create and are strongly perturbed by external fields [7]. However, we have recently demonstrated that quasi-one-dimensional (quasi-1D) very-high-n atoms can be engineered from lower-n quasi-1D atoms using a tailored sequence of HCPs [8]. Here we take advantage of this technique to produce quasi-1D $n \sim 570$ atoms to access the high-scaled-frequency ($\nu_0 \sim 15$) regime. (An alternative route to high scaled frequencies is to use trains of attosecond HCPs produced using high-harmonic generation and two-color laser driving [9]. However, this method, which still remains to be implemented, would yield freely propagating pulses with net zero average field which would lead to a distinctly different atomic dynamics [4].)

In this experimental realization of the true high-frequency limit we use unipolar trains of HCPs with nonvanishing average field to investigate the nonmonotonic decay of the survival probability as a function of the number N of HCPs in the train. Such behavior was initially predicted theoretically for the 1D kicked atom [5]. Under appropriate conditions we observe pronounced structure, the survival probability actually increasing with N over some ranges of N. This behavior contrasts with that seen at lower scaled frequencies, and its physical origins are discussed with the aid of classical trajectory Monte Carlo (CTMC) simulations.

II. REALIZATION OF THE HIGH-SCALED-FREQUENCY REGIME

The present apparatus is described in detail elsewhere [10]. Briefly, potassium atoms in a collimated beam are photoexcited in a weak dc field of $\sim$250 μV cm^{-1} to the lowest-lying redshifted states in the $n=350$, $m=0$ Stark manifold using an extra-cavity doubled Coherent CR699-21 Rh6G dye laser. Excitation results in the creation of a narrow distribution of quasi-1D states with a sizeable scaled dipole moment. In the following it is assumed that the initial quasi-1D state is oriented along the $+z$ axis, i.e., that the z component of the dipole moment $d = -\langle\psi|z|\psi\rangle = -\langle z\rangle$ is negative. If the duration T_p of a HCP with electric-field profile $\vec{F}_{HCP}(t)$ satisfies the condition $T_p \ll T_n$, it simply delivers an impulsive momentum transfer or "kick" to the excited electron given by $\Delta\vec{p} = -\int \vec{F}_{HCP}(t)dt$. (Unless otherwise noted, atomic units are used throughout.) In this work the impulses produced by the HCPs are directed along the z axis either towards or away from the nucleus, i.e., $\Delta\vec{p} = \Delta p\hat{z}$ with $\Delta p < 0$ or $\Delta p > 0$, respectively.

The quasi-1D $n \sim 570$ atoms studied here are created by manipulating $n_i = 350$ quasi-1D atoms using the tailored sequence of HCPs shown in the inset in Fig. 1. The depicted

 ©2006 The American Physical Society

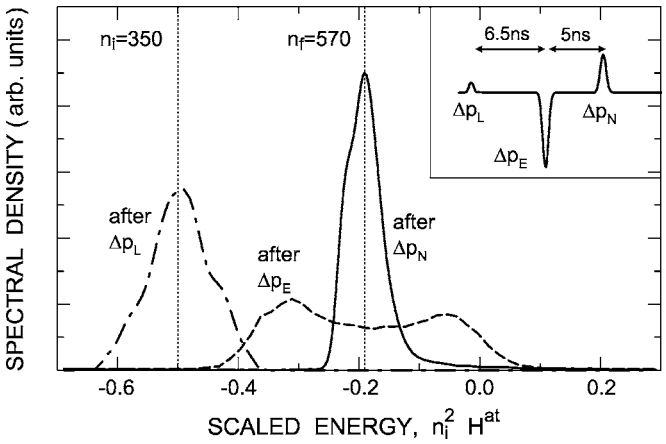

FIG. 1. Evolution of the calculated electron energy distribution, expressed in scaled units, $n_i^2 H^{at}$, during the pulse sequence shown in the inset to quasi-1D n_i=350 states to prepare an elongated n_f =570 states. Distributions are included following application of the localization kick with strength $n_i \Delta p_L = -0.085$, the elongation kick with strength $n_i \Delta p_E = 0.8$, and the narrowing kick of strength $n_i \Delta p_N = -0.404$. Calculations were performed using the experimental pulse profile consisting of a 600-ps pulse followed by two 500-ps pulses. The corresponding peak fields were 58, 448, and 227 mV cm^{-1}, respectively.

protocol is a simplified version of that introduced in Ref. [8] and has the advantage that fewer preparation pulses are required. The first HCP provides a weak "localizing" kick Δp_L of scaled strength $n_i \Delta p_L = -0.085$ directed towards the nucleus. (Note that in this "preparation" phase we scale the kicks to the atomic momentum of the initial state, $1/n_i$. Following preparation of the very-high-n states, the kicks in the subsequent HCP train are scaled to the momentum of the final state, $1/n_f$.) While this kick leads to only small changes in n (see Fig. 1), it creates a wave packet that undergoes periodic focusing into a localized region of phase space near the outer classical turning point [11]. Localization first occurs after a time $t_L \sim 6.5$ ns, i.e., after a scaled time delay $t_L / T_{n_i} \sim 1$. At this time a large "elongation" kick Δp_E of scaled strength $n_i \Delta p_E = 0.8$ is applied directed away from the nucleus. Classically, this impulse transfers the electron to highly eccentric orbits and populates a broad distribution of states with values of n ranging from $n \sim 350$ to the continuum (see Fig. 1). Following a further time delay, $t_D \simeq 5$ ns, a "narrowing" kick with scaled strength $n_i \Delta p_N = -0.404$ is applied directed towards the nucleus to decrease the width of the energy distribution. The size and timing of this kick was optimized using a combination of CTMC simulations and experimental measurements to obtain the narrowest distribution of final n states, i.e., electron energies. (The physical mechanisms responsible for this n narrowing are discussed in Ref. [8].) The computed final electron energy distribution, expressed in scaled units $n_i^2 H^{at}$, is shown in Fig. 1 and corresponds to population of states with a relatively narrow distribution of n (± 40) centered on $n_f \sim 570$. A further delay of ~ 120 ns allows the phase-space distribution to spread and become quasistationary whereupon the atoms are subject to a periodic train of N identical HCPs (see inset in Fig. 2).

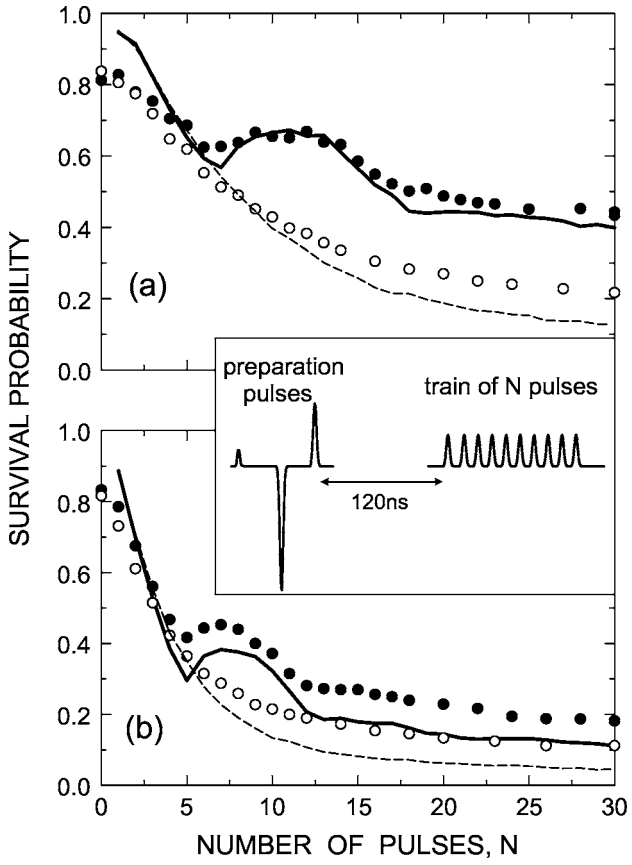

FIG. 2. Dependence of the survival probability on the number N of HCPs in a train of 600-ps-wide HCPs applied after the initial preparation of quasi-1D states with $n_f \sim 570$. The frequency of the train is $\nu_T \sim 500$ MHz (i.e., a scaled frequency $\nu_0 = 2\pi n_f^3 \nu_T \simeq 15$). Results are included for kicks with scaled magnitude $n_f |\Delta p|$ (peak field) of (a) 0.12 (67 mV cm^{-1}) and (b) 0.24 (135 mV cm^{-1}) directed both towards (solid lines and circles) and away from (dashed lines and open circles) the nucleus. Symbols represent experimental data while the lines represent the results of CTMC simulations using the experimentally measured pulse profiles. The inset shows the complete HCP sequence experienced by the atoms.

Experiments are conducted in a pulsed mode. The output of the laser is chopped into a series of pulses of ~ 1 μs duration and ~ 20 kHz pulse repetition frequency using an acousto-optic modulator. The HCP sequence, shown in the inset of Fig. 2, was produced by combining the outputs of several pulse generators and applying them to a nearby electrode. The profiles and amplitudes of the various HCPs were monitored using a fast probe and storage oscilloscope. The width of the individual HCPs is ~ 500 ps full width at half maximum and their peak amplitudes correspond to fields in the range 50–500 mV cm^{-1}. Measurements showed that, whereas the amplitudes and profiles of the pulses forming the train of N HCPs were very similar, the separation between the first pair of pulses in the train was systematically 16% larger than that between succeeding pairs of pulses. (This different spacing is included in the CTMC simulations discussed later.) The number of atoms that survive the HCP sequence is determined using selective field ionization (SFI). Measurements in which no HCPs are applied are interspersed

at routine intervals during data acquisition to monitor the number of Rydberg atoms initially created. The Rydberg atom survival probability is then determined by taking the ratio of the SFI signals observed with and without the HCPs applied.

Figure 2 shows the dependence of the measured survival probabilities on the number N of HCPs in the train for situations where these deliver kicks directed towards and away from the nucleus. The HCPs have a frequency $\nu_T \sim 500$ MHz (i.e., a scaled frequency $\nu_0=\nu_T/\nu_{n_f}\sim 15$) and data are included for scaled kick strengths $\Delta p_0=n_f\Delta p = \pm 0.12$ and ± 0.24. (We use the subindex "0" to denote quantities scaled with respect to n_f.) For kicks directed away from the nucleus the survival probability simply decreases monotonically with increasing N. In contrast, for kicks directed towards the nucleus, the survival probability displays pronounced structure and for certain ranges of N actually increases with N even though in both cases classically chaotic ionization is expected in the high-frequency limit. The values of N at which peaks appear depend on the size of the kicks, i.e., $|\Delta p_0|$, and shift to lower N as $|\Delta p_0|$increases. For all values of N and $|\Delta p_0|$, however, the survival probability is larger than that for kicks directed away from the nucleus. This structure in the survival probability contrasts with the behavior observed at lower scaled frequencies where (for both kick orientations) the survival probability simply decreases steadily as N increases [12].

III. THEORY

Figures 2 and 3 include results predicted using fully three-dimensional (3D) CTMC simulations that follow an ensemble of points in phase space that represent the initial (stationary) Rydberg states. The set of states after laser excitation is taken to be a statistical mixture of 36 oriented Stark states belonging to the $n_i=350$, $m=0$ manifold and centered on the parabolic quantum number $n_1=320$. The ensemble is propagated using Hamilton's equations of motion for the hydrogenic Hamiltonian

$$H=\frac{p^2}{2}-\frac{1}{r}+zF(t)=H^{at}+zF(t), \tag{3.1}$$

where $\vec{r}=(x,y,z)$ and $\vec{p}=(p_x,p_y,p_z)$ denote the position and momentum of the electron, respectively, and $F(t)$ describes the sequence of applied HCPs including those used to prepare the initial very-high-n states. (The use of a K^+ core ion potential did not significantly change the model predictions.) The time-evolved phase-space distribution yields the final electron energy distribution (and its N dependence) from which the overall survival probability can be determined. The calculated survival probabilities in Fig. 2 assume that product states with values of n above the cut off $n_{max} \sim 1000$ are ionized by field inhomogenities present in the apparatus. The calculated survival probability mirrors that observed experimentally. The differences between theory and experiment can be attributed, at least in part, to uncertainties in n_{max} and in the sizes of the kicks delivered by the various HCPs.

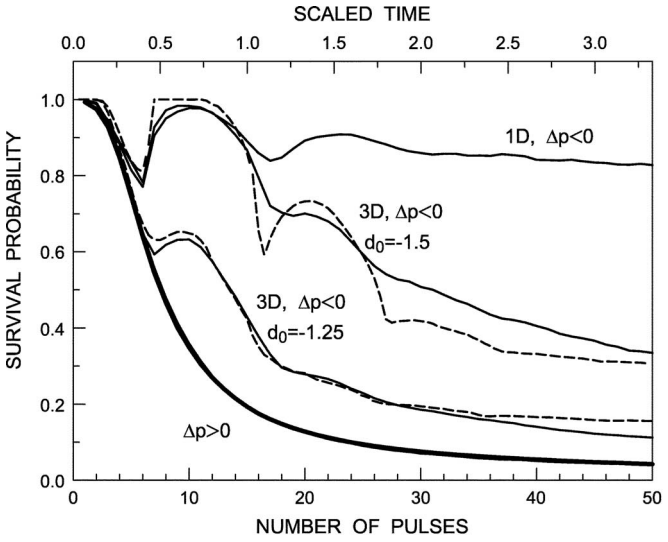

FIG. 3. Solid lines: dependence of the survival probability on the number N of kicks in a perfectly periodic train of kicks applied to $n_f=570$ 1D Rydberg atoms and to quasi-1D Rydberg atoms with $n_f=570$, $m=0$, and $n_1=568$ and 522 (i.e., with scaled dipole moments of $d_0=-1.5$ and $d_0=-1.25$, respectively). Results are presented for a scaled frequency $\nu_0=2\pi n_f^3\nu_T=15$ for kicks with scaled magnitude $n_f|\Delta p|=0.15$ directed both towards and away from the nucleus. Data are also included (dashed lines) for quasi-1D Rydberg atoms subject to a dc field $F^{av}=-\nu_T\Delta p$ (equal to the average field of the train of kicks) suddenly applied at $t=0$. The results for kicks directed away from the nucleus (thick solid line) are essentially independent of the initial state and whether the HCP train is replaced by its average dc field.

Since the measured and calculated nonmonotonic decay of the survival probability is much less pronounced than that predicted for 1D kicked atoms [5], it is of interest to compare the results in Fig. 2 with those for simpler 1D and 3D systems. To this end, we display in Fig. 3 survival probabilities for specific 1D and quasi-1D $n_f=570$ states subject to a strictly periodic train of ultrashort kicks,

$$F'(t)=-\Delta p\sum_{k=1}^{N}\delta(t-k\nu_T^{-1}). \tag{3.2}$$

with $|\Delta p_0|=n_f|\Delta p|=0.15$ and $\nu_0=\nu_T/\nu_{n_f}=15$. In each case the survival probability exhibits nonmonotonic decay when the kicks are directed towards the nucleus (i.e., $\Delta p<0$). The decay rate depends markedly on the polarization of the initial state and the survival probability for the parabolic state ($n_1=522$) with initial scaled dipole moment $d_0=n_f^2 d=-1.25$ is very similar to that seen in Fig. 2. Since in the 1D system electrons trying to leave the nucleus along the positive z axis are kicked back towards the nucleus, the survival probability decreases only slowly. The results for the extreme parabolic state (i.e., $n_1=568$, $d_0=-1.5$) mimic the 1D result at early times (up to ~ 12 kicks). However, the 3D and 1D results eventually diverge because in the 3D system the electron can explore a larger phase space and leave the atom (in the direction of the kicks) along the negative z axis. Remarkably for kicks directed away from the nucleus ($\Delta p>0$), the 1D

and 3D results are essentially identical and independent of the dipole moment of the initial state. In this case the dynamics is clearly quasi-one-dimensional.

In the limit $\nu_0 \rightarrow \infty$ the dynamics of the kicked Rydberg atom should approach that of the Rydberg atom for the Stark Hamiltonian,

$$H^{Stark} = H^{at} + zF^{av}, \tag{3.3}$$

where $F^{av} = -\nu_T \Delta p$ is the average dc field associated with the HCP train. This follows from the observation that the electron can respond only to the zero-frequency component of the train of kicks (i.e., the field F^{av}) because all other Fourier components are too fast for the electron to react to. The survival probability for Rydberg atoms initially in $n_f = 570$ states and subject to a dc field $F^{av} = -\nu_T \Delta p$, that is suddenly switched on at $t = 0$ and turned off at the end of the last kick, is included in Fig. 3. (The upper scale for the abscissa in the figure shows the scaled turn-off time.) The behavior of the survival probability is very similar to that for the kicked atom, indicating that this behavior is directly related to the dynamics of Rydberg electrons in a dc field. In fact, similar behavior has been reported theoretically and experimentally for Rydberg atoms subject to long HCPs of variable duration [10,13]. Figure 3 indicates that the first minimum in the survival probability occurs at a time slightly less than half of the period of the initial $n_f = 570$ states, much like the behavior reported in Refs. [10,13]. The classical nonmonotonic behavior of the survival probability governed by the Stark Hamiltonian has been found to agree, for lower n levels, with the behavior of the quantum coherent superposition of states created by sudden application of the dc field [13].

The origin of the nonmonotonic decay of the survival probability follows from the evolution of the electron energy distribution as the number N of HCPs in the train is increased, which is shown in Fig. 4 for representative kick strengths and directions. For kicks of scaled strength $\Delta p_0 = 0.12$ directed away from the nucleus, i.e., in the $+z$ direction [Fig. 4(a)], the energy distribution broadens and shifts towards positive energies as N increases. This results because electrons initially moving towards the nucleus are slowed by a kick and lose energy whereas those initially moving away from the nucleus are accelerated and gain energy, quickly escaping the atom. Eventually those electrons traveling towards the nucleus reverse direction whereupon they are accelerated and leave the atom. As is evident from Figs. 4(b) and 4(c), the situation is quite different if the kicks are directed towards the nucleus, i.e., in the $-z$ direction. The energy distribution develops ripples in the form of outgoing waves, which are directly responsible for the nonmonotonic decay of the survival probability. The formation of wavelike structures can be understood with the aid of the representative classical electron trajectories depicted in Figs. 5(a)–5(c) which lead to ionization after single, double, and triple scattering events at the nucleus, respectively.

As is evident from the data in Fig. 4(b) (for $|\Delta p_0| = 0.12$), as N increases the electron energy distribution first broadens. After about half an orbital period ($N \sim 7$), the electron energy distribution comprises two distinct peaks: one centered at a scaled energy of $H_0^{at} \simeq -0.58$, the other near $H_0^{at} \sim 0$. The

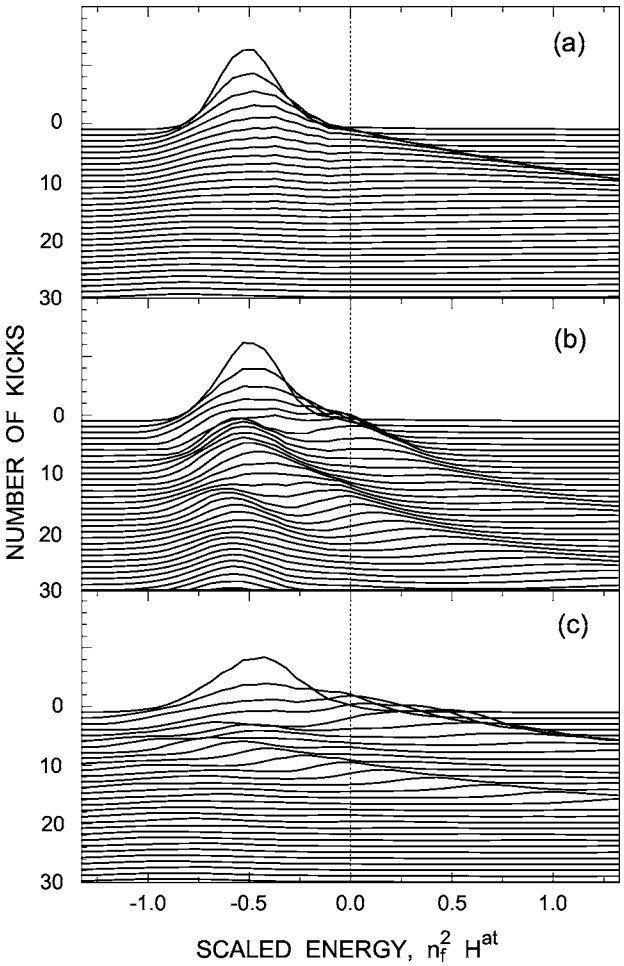

FIG. 4. Calculated evolution of the electron energy distribution using the experimental pulse profile as the number N of HCPs in the train is increased. Results are presented for kicks with scaled magnitude $n_f|\Delta p| = 0.12$ directed (a) away from and (b) towards the nucleus, and (c) for kicks of magnitude $n_f|\Delta p| = 0.24$ directed towards the nucleus.

latter feature is associated with electrons accelerated towards the nucleus where they are only slightly deflected. These electrons continue with a negative z component of velocity and are accelerated by successive pulses passing further into the continuum and escaping [see Fig. 5(a)]. Those electrons that backscatter at the nucleus [see Figs. 5(b) and 5(c)] acquire a positive z component of velocity. Subsequent kicks lead to a loss of energy resulting in the small increase in survival probability evident in Fig. 2(a) following $N \sim 7$ kicks. (The use of larger kicks, $|\Delta p_0| = 0.24$, leads to stronger acceleration towards the core ion and scattering becomes important following fewer kicks. This is apparent in the evolution of the corresponding electron energy distribution shown in Fig. 4(c) and in Fig. 2(b) where the survival probability is seen to increase following $N \sim 5$ kicks.) The subset of trajectories that initially move away from the core ion and lose energy due to the kicks eventually reach their outer turning points and are accelerated back towards the core ion where they undergo scattering. The calculations indicate that following $N \sim 15$ kicks the distribution then begins to acquire a secondary higher-energy ripple that subsequently passes into

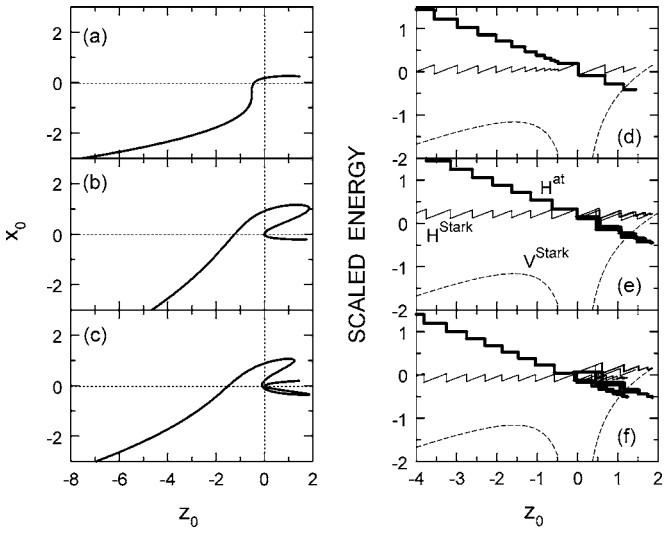

FIG. 5. (a)–(c) Typical ionizing trajectories in the x-z plane for electrons that undergo single, double, and triple scattering events at the nucleus (located at the origin) prior to leaving the atom. (d)–(f) Time evolution of the scaled atomic (thick solid lines) and Stark energies (thin solid lines) in the energy-z plane corresponding to the trajectories in (a)–(c), respectively. The dashed lines illustrate the Stark potential $V^{Stark}=-1/|z|+F^{av}z$ that approximately governs the dynamics of the electron.

the continuum. This process repeats but becomes increasingly difficult to detect because of the broadening of the energy distribution (i.e., the orbital period distribution) and the reduction in the number of surviving bound states. No clear maximum in survival probability associated with this secondary peak is observed in Fig. 2 but it is evident in Fig. 3 for the more strongly polarized initial states. For values of $N>30$ the electron energy distribution changes little and is comprised of a single broad peak centered near $n\sim 450$.

The rapid decrease in the survival probability with increasing number of kicks is due to the large value of the average dc Stark field associated with the HCP train, which is given in scaled units by $F_0^{av}=0.36$. The presence of this field leads to the appearance of a saddle point in the effective potential (shown in Fig. 5) across which ionization eventually proceeds. The initial average Stark energy of the electron $\langle H_0^{Stark}\rangle=-0.5-F_0^{av}d_0\simeq 0$ lies above the barrier. For positive kicks, electrons initially traveling in the $+z$ direction or backscattered into the $z>0$ region at the nucleus are rapidly accelerated away from the parent atom by successive HCPs. For negative kicks the Stark saddle point is located on the $-z$ axis, and electron escape, which must occur along the $-z$ axis, is transiently suppressed by scattering at the core ion leading to larger overall survival probabilities. The fact that the Stark energy of the individual trajectories in Fig. 5 is approximately conserved illustrates that the dynamics is approximately governed by the Stark Hamiltonian (3.3). The jigsaw motion of the energies is due to the jumps they undergo after every kick. Small deviations from a horizontal line for the Stark energy are a direct measure for the residual influence of the high (but finite) Fourier components of the HCP train. Only in the limit $\nu_0\rightarrow\infty$ would the horizontal line associated with the Stark Hamiltonian be fully recovered. The main effect of the higher Fourier components is to damp the oscillations in the survival probability (see Fig. 3) due to the decrease in the statistical coherence of the electron wave packet.

IV. CONCLUSIONS

This work extends experimental studies of the kicked Rydberg atom to high scaled frequencies. It is shown that under appropriate conditions the survival probability becomes a nonmonotonic, oscillatory function of the number of kicks, N. This results from a wavelike pattern in the two-dimensional probability density $\rho(H^{at},N)$. In the high-frequency limit the dynamics of the kicked Rydberg atom mimics closely that of a Rydberg atom in a dc field equal to the average dc field of the train of pulses. The ability to undertake measurements at high scaled frequencies opens up an interesting regime in which to study the dynamical response of atomic systems and to investigate quantum localization.

ACKNOWLEDGMENTS

This research was supported by the NSF under Grant No. PHY-0353424 and by the Robert A. Welch Foundation. C.O.R. acknowledges support by the OBES, US DOE to ORNL which is managed by the UT-Batelle LLC under Contract No. DE-AC05-00OR22725. S.Y. and J.B. acknowledge support by the FWF (Austria). J.C.L. acknowledges support from the Office of Naval Research.

[1] R. Blümel and U. Smilansky, Phys. Rev. A **30**, 1040 (1984).
[2] C. F. Hillermeier, R. Blümel, and U. Smilansky, Phys. Rev. A **45**, 3486 (1992).
[3] C. O. Reinhold, J. Burgdörfer, M. T. Frey, and F. B. Dunning, Phys. Rev. Lett. **79**, 5226 (1997); M. T. Frey, F. B. Dunning, C. O. Reinhold, S. Yoshida, and J. Burgdörfer, Phys. Rev. A **59**, 1434 (1999).
[4] W. Zhao, J. C. Lancaster, F. B. Dunning, C. O. Reinhold, and J. Burgdörfer, J. Phys. B **38**, S191 (2005).
[5] S. Yoshida, C. O. Reinhold, and J. Burgdörfer, Phys. Rev. Lett. **84**, 2602 (2000); S. Yoshida, C. O. Reinhold, P. Kristöfel, and J. Burgdörfer, Phys. Rev. A **62**, 023408 (2000).
[6] E. Persson, S. Yoshida, X.-M. Tong, C. O. Reinhold, and J. Burgdörfer, Phys. Rev. A **68**, 063406 (2003).
[7] T. F. Gallagher, *Rydberg Atoms* (Cambridge University Press, New York, 1992).
[8] W. Zhao, J. J. Mestayer, J. C. Lancaster, F. B. Dunning, C. O. Reinhold, S. Yoshida, and J. Burgdörfer, Phys. Rev. Lett. **95**, 163007 (2005).
[9] E. Persson, S. Puschkarski, X. M. Tong, and J. Burgdörfer,

Ultrafast Optics, edited by F. Krausz, G. Korn, P. Corkum, and I. A. Walmsley, Springer Series in Optical Sciences Vol. 95, (Springer, Berlin, 2004), pp. 251.

[10] C. L. Stokely, J. C. Lancaster, F. B. Dunning, D. G. Arbó, C. O. Reinhold, and J. Burgdörfer, Phys. Rev. A **67**, 013403 (2003).

[11] D. G. Arbó, C. O. Reinhold, J. Burgdörfer, A. K. Pattanayak, C. L. Stokely, W. Zhao, J. C. Lancaster, and F. B. Dunning, Phys. Rev. A **67**, 063401 (2003).

[12] C. O. Reinhold, W. Zhao, J. C. Lancaster, F. B. Dunning, E. Persson, D. G. Arbo, S. Yoshida, and J. Burgdörfer, Phys. Rev. A **70**, 033402 (2004).

[13] C. O. Reinhold, J. Burgdörfer, R. R. Jones, C. Raman, and P. H. Bucksbaum, J. Phys. B **28**, L457 (1995).